ESC European Society of Cardiology

European Heart Journal Open (2023) **3**, 1–11
https://doi.org/10.1093/ehjopen/oead038

ORIGINAL ARTICLE
Vascular and cardiac imaging

Heterogeneous plaque–lumen geometry is associated with major adverse cardiovascular events

Sophie Z. Gu [1], Yuan Huang[2,3], Charis Costopoulos[4], Benn Jessney[1], Christos Bourantas[5], Zhongzhao Teng[6,7], Sylvain Losdat[8], Akiko Maehara [9], Lorenz Räber [10], Gregg W. Stone[11], and Martin R. Bennett[1,*]

[1]Section of CardioRespiratory Medicine, University of Cambridge, Heart & Lung Research Institute, Papworth Road, Cambridge Biomedical Campus, Cambridge CB2 0BB, UK; [2]Centre for Mathematical and Statistical Analysis of Multimodal Imaging, University of Cambridge, 20 Clarkson Road, Cambridge CB3 0EH, UK; [3]Department of Radiology, University of Cambridge, Addenbrooke's Hospital, Hills Road, Cambridge CB2 0QQ, UK; [4]Department of Cardiology, Royal Papworth Hospital, Papworth Road, Cambridge CB2 0AY, UK; [5]Institute of Cardiovascular Sciences, University College London, 62 Huntley Street, London WC1E 6DD, UK; [6]Tenoke Ltd., Cambridge Biomedical Campus, Hills Road, Cambridge CB2 0AH, UK; [7]Nanjing Jingsan Medical Science and Technology Ltd., 6 Shui You Gang, Nanjing, Jiangsu 210013, China; [8]Institute of Social and Preventive Medicine and Clinical Trials Unit, University of Bern, Hochschulstrasse 6, 3012 Bern, Switzerland; [9]Cardiovascular Research Foundation, 1700 Broadway, New York, NY 10019, USA; [10]Department of Cardiology, Bern University Hospital, Freiburgstrasse 18, 3010 Bern, Switzerland; and [11]The Zena and Michael A. Wiener Cardiovascular Institute, Icahn School of Medicine at Mount Sinai, 1190 Fifth Avenue, New York, NY 10029, USA

Received 23 September 2022; revised 14 March 2023; accepted 12 April 2023; online publish-ahead-of-print 13 April 2023

Handling Editor: Alessia Gimelli

Aims

Prospective studies show that only a minority of plaques with higher risk features develop future major adverse cardiovascular events (MACE), indicating the need for more predictive markers. Biomechanical estimates such as plaque structural stress (PSS) improve risk prediction but require expert analysis. In contrast, complex and asymmetric coronary geometry is associated with both unstable presentation and high PSS, and can be estimated quickly from imaging. We examined whether plaque–lumen geometric heterogeneity evaluated from intravascular ultrasound affects MACE and incorporating geometric parameters enhances plaque risk stratification.

Methods and results

We examined plaque–lumen curvature, irregularity, lumen aspect ratio (LAR), roughness, PSS, and their heterogeneity indices (HIs) in 44 non-culprit lesions (NCLs) associated with MACE and 84 propensity-matched no-MACE-NCLs from the PROSPECT study. Plaque geometry HI were increased in MACE-NCLs vs. no-MACE-NCLs across whole plaque and peri-minimal luminal area (MLA) segments (HI curvature: adjusted $P = 0.024$; HI irregularity: adjusted $P = 0.002$; HI LAR: adjusted $P = 0.002$; HI roughness: adjusted $P = 0.004$). Peri-MLA HI roughness was an independent predictor of MACE (hazard ratio: 3.21, $P < 0.001$). Inclusion of HI roughness significantly improved the identification of MACE-NCLs in thin-cap fibroatheromas (TCFA, $P < 0.001$), or with MLA ≤ 4 mm^2 ($P < 0.001$), or plaque burden (PB) $\geq 70\%$ ($P < 0.001$), and further improved the ability of PSS to identify MACE-NCLs in TCFA ($P = 0.008$), or with MLA ≤ 4 mm^2 ($P = 0.047$), and PB $\geq 70\%$ ($P = 0.003$) lesions.

Conclusion

Plaque–lumen geometric heterogeneity is increased in MACE vs. no-MACE-NCLs, and inclusion of geometric heterogeneity improves the ability of imaging to predict MACE. Assessment of geometric parameters may provide a simple method of plaque risk stratification.

* Corresponding author. Tel: +44 1223 331504, Fax: +44 1223 331505, Email: mrb24@medschl.cam.ac.uk

Graphical Abstract

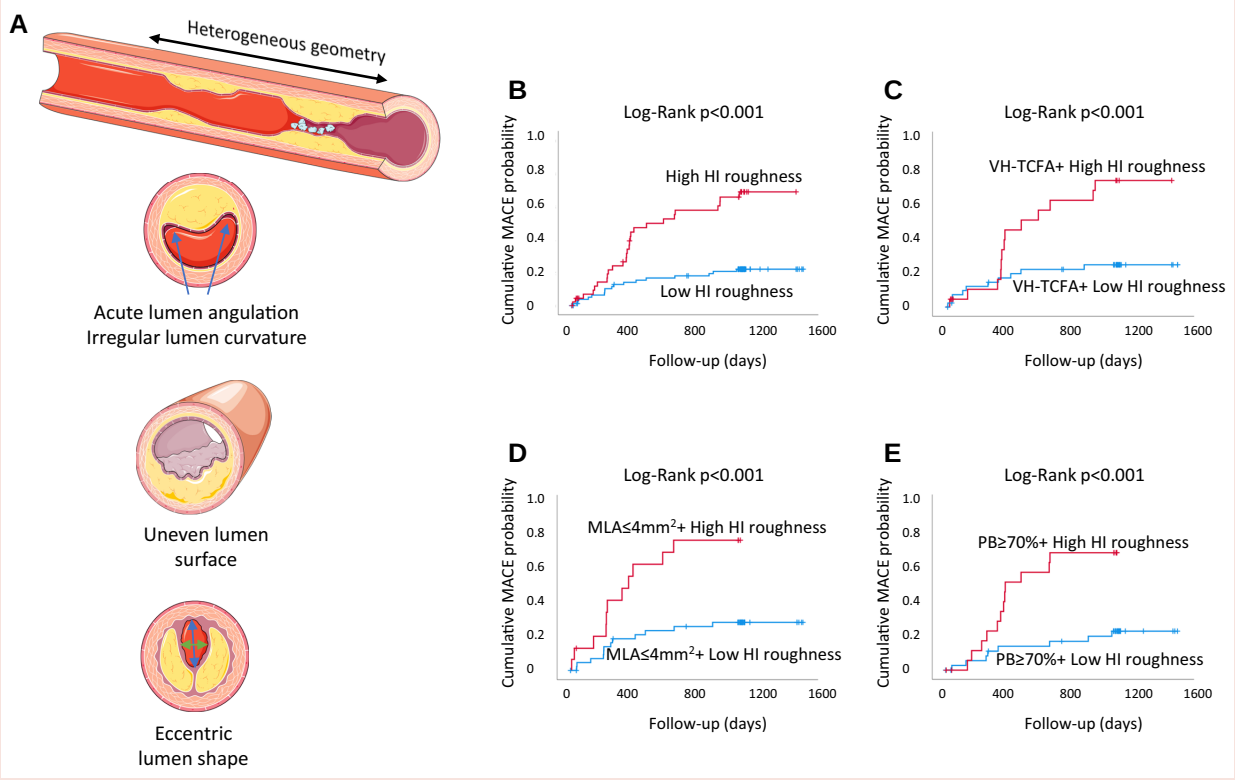

High heterogeneity of plaque–lumen geometry is associated with MACE. (*A*) Schematic illustration of plaque–lumen interface geometric parameters and their longitudinal variation. (*B–E*) Incorporating heterogeneity index (HI) for roughness improves MACE prediction in (*B*) all plaques, (*C*) VH-TCFA, (*D*) MLA $\leq$ 4mm^2, and (*E*) PB $\geq$ 70%. MACE, major adverse cardiovascular events; MLA, minimum luminal area; PB, plaque burden; VH-TCFA, virtual histology thin cap fibroatheroma.

Keywords Intravascular imaging • Major adverse cardiovascular events • Plaque geometry

Introduction

Pathological and coronary imaging studies have identified features of plaques that are more likely to lead to major adverse cardiovascular events (MACE), including large plaque burden (PB) at a severe stenosis, positive arterial remodelling, thin fibrous cap infiltrated with macrophages, large necrotic core, calcified nodules, and spotty calcification.[1,2] Despite these findings, the predictive accuracy of individual higher risk features on single modality imaging is generally low. For example, hazard ratios (HRs) for higher risk plaque features were between 2.0 and 8.1[3–5] from virtual histology intravascular ultrasound (VH-IVUS), 2.1 and 4.7[6,7] from optical coherence tomography (OCT), and 1.9[8] from near-infrared spectroscopy. MACE rates are low with low test positive predictive values (PPV) ranging between 13 and 41% in these studies,[9] and while combinations of features improve predictive accuracy, lesion numbers having more features reduces dramatically. These limitations of conventional plaque structural features, composition, and lumen stenosis have identified the need for additional parameters to predict risk, including those based on biomechanics and plaque geometry.

Plaque–lumen morphology represents the inner lumen/plaque interface and may be an important indicator of vulnerability that can be defined by multiple modalities. For example, an irregular lumen surface on OCT or longitudinal lesion asymmetry on angiography is associated with acute coronary syndrome (ACS) presentation and increased risk of plaque instability,[10,11] while complex coronary lesion geometry affects the functional significance of coronary stenoses.[12] Changes in lesion geometry detected on OCT can also be due to silent rupture and plaque healing that leads to rapid plaque growth.[6,13] Conversely, changes in luminal geometric parameters have been reported following intensive lipid lowering.[14]

While an irregular luminal surface may indicate risk of plaque rupture or growth, the precise parameters and their mechanism of action are not known, and asymmetry or heterogeneity of parameters may be more important than the parameters themselves. For example, longitudinal lesion asymmetry affects location of plaque rupture sites, clinical presentation,[11] lesion eccentricity, and regional distribution of plaque structural stress (PSS).[15,16] High PSS can affect plaque growth and composition,[17] and is more heterogeneous in plaques that lead to MACE.[18] However, PSS calculation requires high computational cost and long simulation time. A surrogate marker achievable by fast processing is urgently needed. We therefore examined: (i) plaque geometric parameters and their heterogeneity in non-culprit lesion (NCL) MACE plaques compared with a propensity-score-matched control population; (ii) if incorporating geometric parameters enhances MACE prediction over intravascular imaging alone; and (iii) the relationship between plaque geometry and PSS.

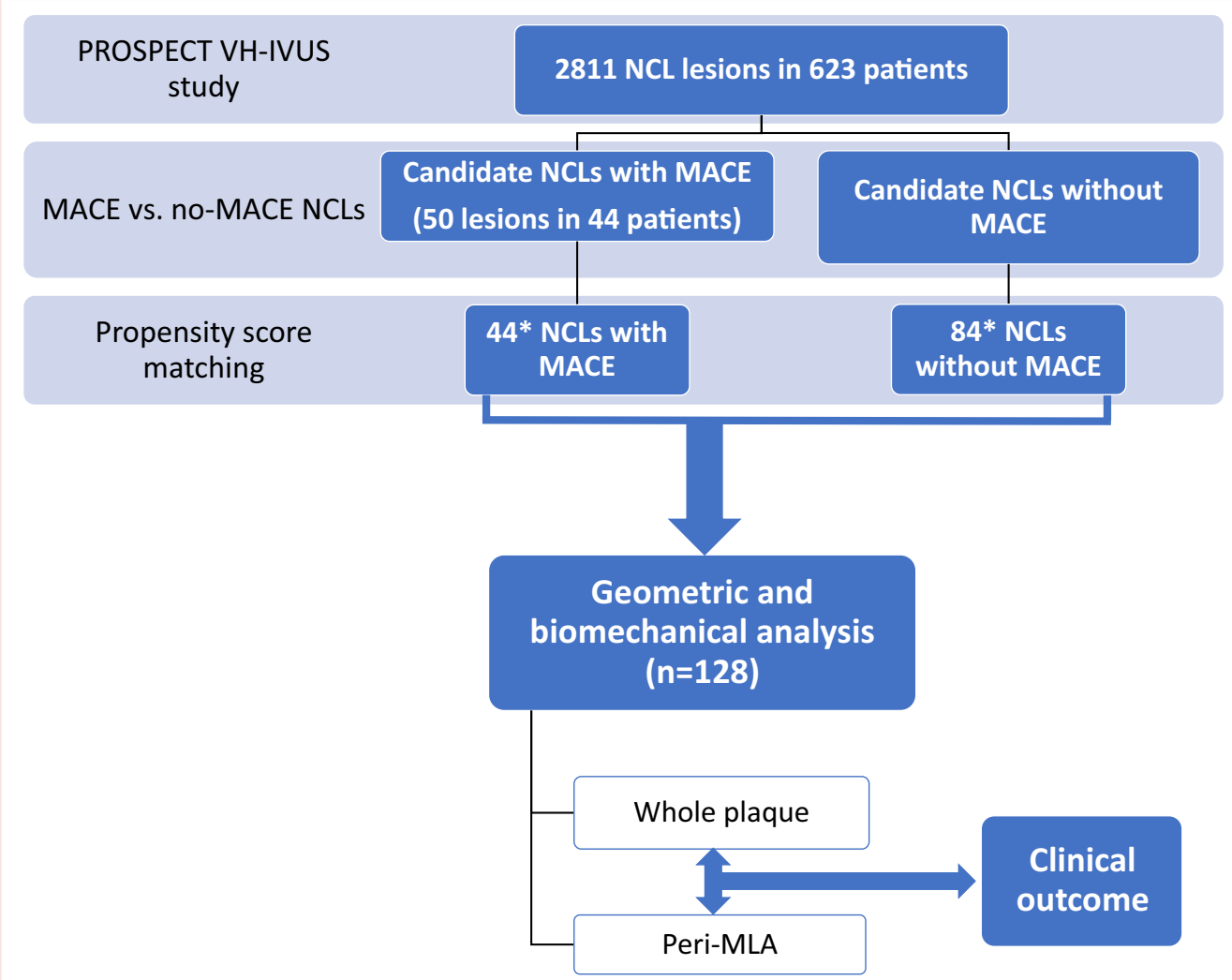

Figure 1 Study flow chart. Schematic representation of plaques included from the PROSPECT study with clinical outcome measures. MACE, major adverse cardiovascular events; MLA, minimal luminal area; NCL, non-culprit lesion; PB, plaque burden; VH-IVUS, virtual histology intravascular ultrasound. *1 lesion per patient, total patients, 128.

Methods

Study population

Plaque geometric parameters and their heterogeneity were examined by a *post-hoc* analysis of the Providing Regional Observations to Study Predictors of Events in the Coronary Tree (PROSPECT) study, a prospective multicentre natural history study to identify plaque features that cause MACE. Study design, definitions, endpoints, inclusion, and exclusion criteria are described elsewhere.[3] The study was approved by the Institutional Review Boards (ClinicalTrials.gov: NCT00180466) and all patients provided informed consent. Briefly, 697 patients with ACS underwent three-vessel VH-IVUS imaging after successful intervention in all flow-limiting lesions, and followed up for a median of 3.4 years. Primary endpoints were NCL MACE, defined as cardiac death, myocardial infarction (MI), or rehospitalization due to progressive or unstable angina, adjudicated by a clinical events committee with no knowledge of other patient data. Clinical events were attributed to culprit lesions or NCLs based on follow-up angiography. One hundred and four NCLs developed subsequent MACE but only 50 lesions from 44 patients had baseline VH-IVUS imaging. Only one lesion per patient was selected. In patients with multiple NCLs, the lesion with the greatest PB was chosen. We therefore compared 44 patients who experienced an NCL MACE against 84 propensity-matched patients who did not (*Figure 1*).

Virtual histology intravascular ultrasound image acquisition and analysis

VH-IVUS was performed using a 20 MHz synthetic aperture array 3.2-F catheter (Eagle Eye, In-Vision Gold, Volcano, Rancho Cordova, California) with motorized pullback at 0.5 mm/s. An independent core laboratory (Cardiovascular Research Foundation, New York) undertook VH-IVUS segmentation at every end-diastolic frame, including lumen and external elastic membrane area, plaque area, PB, and composition (fibrotic, fibrofatty, calcific and necrotic core area, and percentage). Plaques were defined as ≥3 consecutive frames with PB ≥ 40% and classified as virtual histology thin-cap fibroatheroma (VH-TCFA), virtual histology thick-cap fibroatheroma, virtual histology pathological intimal thickening, virtual histology fibrotic, or virtual histology fibrocalcific plaque as previously described.[3] Minimal luminal area (MLA) was defined as the IVUS frame with the smallest luminal area over the whole plaque. If PB at the MLA site was ≥70%, the lesion was

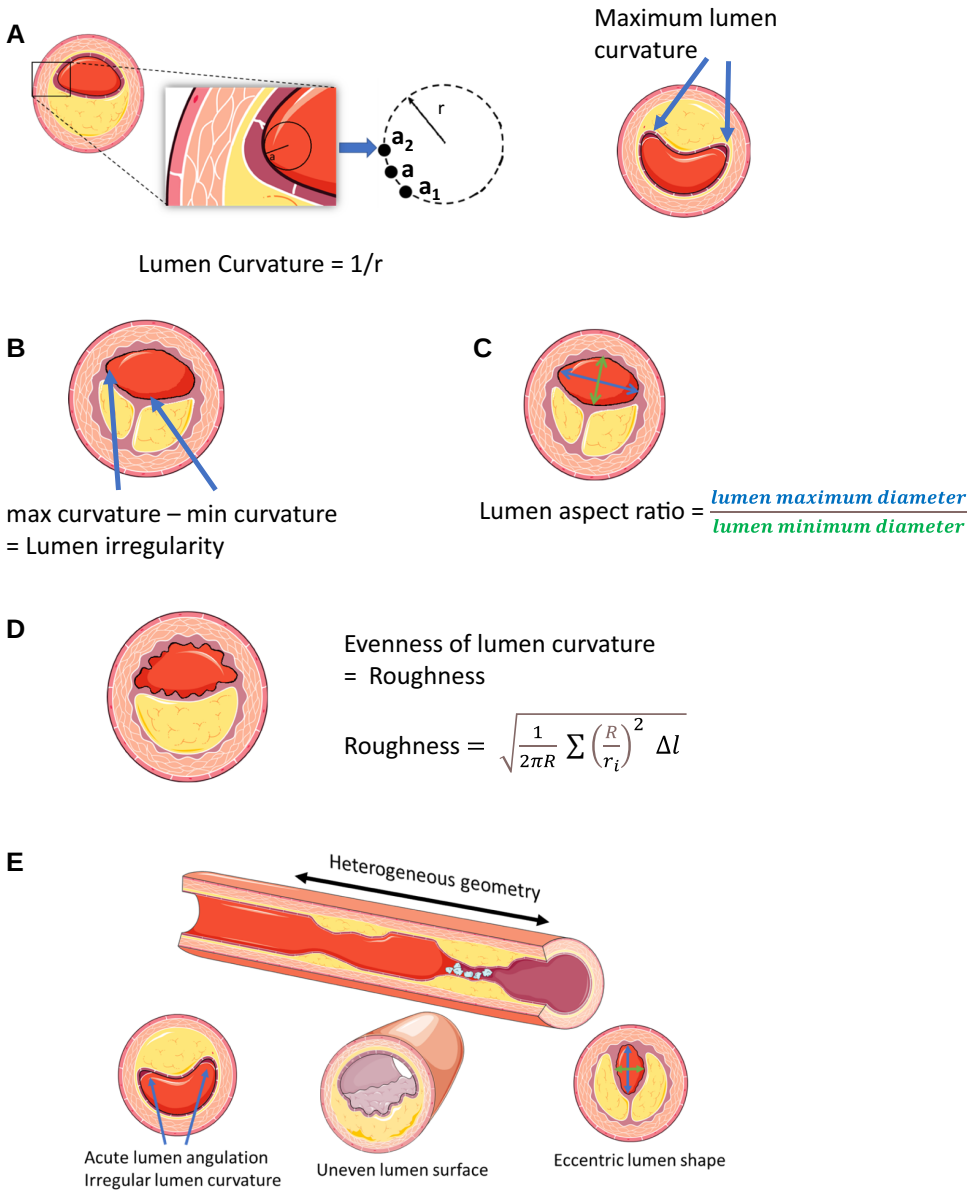

Figure 2 Geometric parameter assessment. (*A*) Lumen curvature: curvature at point **a** was computed using the radius (*r*) of the circle determined by point **a** and two adjacent points ($\mathbf{a_1}$ and $\mathbf{a_2}$), i.e. lumen curvature = 1/*r*, (*B*) lumen irregularity: measure of variation of lumen curvature, (*C*) lumen aspect ratio: measure of lumen shape, (*D*) lumen roughness: measure of evenness of lumen curvature. *R* is the radius of the circle best fitting the lumen contour (i.e. lumen area=πR^2), r_i is the radius used to calculate curvature at point *i*, Δl is the half distance of the curve connecting $i-1^{th}$, i^{th}, and $i+1^{th}$ points. (*E*) Schematic illustration of plaque–lumen interface geometric parameters and their longitudinal variation.

classified as having PB ≥ 70%. Analysis was performed off-line and not used for procedural guidance.

Geometric and biomechanical analysis

Vessel geometry and plaque composition were extracted from VH-IVUS data and imported into dedicated analysis software (proprietary code, MATLAB R2022b, MathWorks, Inc., Natick, MA). Geometric parameters were assessed for every VH-IVUS frame as described previously[14] and summarized below and in *Figure 2* (for further details see Supplementary material online). Core laboratory lumen segmentation was used to calculate geometric parameters and performed blinded to patient clinical data.

- **Lumen curvature**: reflects lumen angulation. Curvature values were computed for all points (~200 data points) in the lumen.
- **Lumen irregularity**: defined as difference between maximum and minimum curvature.
- **Lumen aspect ratio (LAR)**: reflects lumen shape and is calculated as ratio of maximum to minimum diameter of ellipse, i.e. lower LAR describes a rounder lumen, and a value of 1 indicates a perfectly circular lumen.
- **Lumen roughness**: reflects lumen surface evenness in respect to curvature, and is calculated using the formula in *Figure 2D*, with smaller values representing more round or even surface. A perfect smooth and round lumen shape will have roughness of 1.

Frames containing side branches or immediately adjacent to bifurcations were excluded as they violated the plane strain assumption for 2D solids. Vessel geometry and plaque composition were extracted to allow construction of 2D solid models, and 2D dynamic finite element analysis was performed to calculate PSS as described previously (see Supplementary material online).[16,17] Maximum principal stress in the peri-luminal region was used to indicate critical mechanical conditions within the structure.

Statistical analysis

Propensity score matching can be found in Supplementary material online. Data variables are presented as mean ± standard deviation (SD), or median (interquartile range). Numerical variables were compared using Mann–Whitney *U* tests and categorical variables using χ^2 tests. Outliers were removed using the median absolute deviation method with threshold 3.5. As each plaque had multiple VH-IVUS frames, linear mixed-effects models were used to account for hierarchical data structure and clustering in individual patients with results presented as mean ± standard error (SE). Adjustment of *P* values for multiple comparisons was performed using the Bonferroni method. Model diagnostics were performed by inspecting residual and Q–Q plots to test model assumptions. Association between continuous variables was assessed by Pearson's correlation coefficient and linear regression. Receiver operating characteristics curve analysis was performed for lumen geometric variables to identify best cut-off that predicted MACE using Youden index, which was used to categorize geometric heterogeneity into low and high groups, allowing generation of time-to-event curves. Time-to-event data are presented as Kaplan–Meier estimates of cumulative hazard and compared using the log-rank method. Cox regression analysis was used to identify individual lumen geometric, and PSS predictors of MACE, and all statistically significant variables entered into a multivariable model to identify independent predictors; non-significant variables were excluded by backward logistic regression selection. Proportional hazards assumption was tested by checking the interaction between the time measure and covariates. Statistical significance was indicated by two-tailed $P < 0.05$. Analyses were performed in SPSS (version 27, IBM, New York) and R (version 4.2.2, R Foundation for Statistical Computing, Vienna).

Results

Patient and lesion characteristics

Baseline clinical characteristics were similar between the two groups, including age, sex, cardiovascular risk factors, or clinical presentation (see Supplementary material online, *Table S1*). Forty-four events included: 3 MI, 13 unstable angina, and 28 rehospitalization (25 led to revascularization) due to progressive angina. VH-TCFA was the predominant lesion phenotype in both MACE and no-MACE groups (52.3 vs. 47.6%; $P = 0.617$), and MLA, PB, and composition were also similar.

Heterogeneity of geometric parameters is increased in non-culprit lesions associated with major adverse cardiovascular events at peri-minimal luminal area segments

Geometric parameters and PSS and their longitudinal heterogeneity over each plaque were examined, with the heterogeneity index (HI) defined as the standard deviation divided by the mean of each parameter. As MLA ≤ 4 mm^2 is a higher risk feature for future MACE,[3,4] both whole plaque (median lesion length 24.1 mm) and peri-MLA segments (4 mm proximal and distal to the MLA) were analysed. The computational time for peri-MLA geometric analysis was 11.5 ± 5.5 min compared with PSS assessment 190 ± 153 min.

Multiple geometric parameters and PSS and their longitudinal heterogeneity were determined in 9060 VH-IVUS frames ($n = 3115$ MACE, $n = 5945$ no-MACE). There were no differences in geometric parameters, PSS, or their HI between male and female patients (see Supplementary material online, *Table S2*). Maximum curvature, irregularity, LAR, and roughness were similar between MACE and no-MACE groups at both whole plaque and peri-MLA segments (*Figure 3A–D*). However, plaques showed heterogeneous longitudinal geometries across the whole plaque and peri-MLA segments. The HI of the geometric parameters, a measure of the variation of each parameter between frames, was increased in two of four parameters in MACE vs. no-MACE plaques across the whole plaque (HI curvature$_{max}$: 0.23 ± 0.01 vs. 0.22 ± 0.01, adjusted $P = 0.072$; HI irregularity: 0.37 ± 0.01 vs. 0.32 ± 0.01, adjusted $P = 0.008$; HI LAR: 0.086 ± 0.003 vs. 0.075 ± 0.002, adjusted $P = 0.016$; HI roughness: 0.046 ± 0.003 vs. 0.039 ± 0.002, adjusted $P = 0.116$), and for all parameters in the peri-MLA regions (HI curvature$_{max}$: 0.21 ± 0.01 vs. 0.18 ± 0.01, adjusted $P = 0.024$; HI irregularity: 0.34 ± 0.02 vs. 0.27 ± 0.01, adjusted $P = 0.002$; HI LAR: 0.08 ± 0.004 vs. 0.06 ± 0.003, adjusted $P = 0.002$; HI roughness: 0.044 ± 0.004 vs. 0.031 ± 0.002, adjusted $P = 0.004$). No significant differences were found for all parameters between MACE whole plaque and peri-MLA regions.

High peri-minimal luminal area roughness heterogeneity is an independent predictor of future major adverse cardiovascular events

PROSPECT identified that VH-TCFAs, MLA ≤ 4 mm^2, and PB ≥ 70% at the MLA site were associated with future NCL MACE. However, their predictive value was limited as ∼50% of lesions without these features also resulted in MACE (45.5% NCL MACE plaques with MLA > 4 mm^2, 54.5% with PB < 70% at MLA, and 49.0% with non-VH-TCFA). We therefore examined whether geometric parameter heterogeneity can predict MACE. We focused this analysis on peri-MLA segments since both HI PSS[18] and HI of the geometric parameters (*Figure 3*) were more consistently associated with MACE at peri-MLA segments than the whole lesion, and a focused analysis over a shorter distance at peri-MLA regions allows faster and easier assessment.

MACE rates were higher for plaques with high HI curvature (threshold = 0.172, $P = 0.006$), irregularity (threshold = 0.274, $P < 0.001$), LAR (threshold = 0.074, $P < 0.001$), and roughness (threshold = 0.035, $P < 0.001$, *Figure 4*). Heterogeneity indices for all geometric parameters were associated with NCL MACE on univariate analysis (*Table 1*). All geometric parameters were entered into the multivariate regression model, high HI roughness [HR: 3.21, 95% confidence interval (CI) 1.70–6.05, $P < 0.001$], and high HI of PSS$_{max}$ (HR: 2.67, 95% CI 1.40–5.10, $P = 0.003$) were independent predictors of MACE. HI roughness provided superior specificity compared with VH-IVUS features (HI roughness = 77.4%, VH-TCFA = 52.4%, MLA ≤ 4 mm^2 = 57.1%, PB ≥ 70% = 57.1%), while offering higher sensitivity (HI roughness = 61.4%, TCFA = 52.3%, MLA ≤ 4 mm^2 = 52.3%, PB ≥ 70% = 45.5%).

Maximum curvature, lumen aspect ratio, and roughness correlate with plaque structural stress

PSS and heterogeneity of PSS are associated with MACE,[18] possibly due to marked differences in PSS causing unequal displacement of heterogeneous tissues. We therefore examined correlations between geometric parameters and PSS and their heterogeneity on whole plaques. Maximum curvature, LAR, and roughness (but not irregularity) were positively correlated with PSS$_{max}$ (see Supplementary material online, *Table S3*), while correlations between HI curvature, irregularity, LAR, roughness, and HI of PSS$_{max}$ were mostly much stronger, and all significant. Together these data show that although HI roughness and HI PSS are positively correlated, they are independent predictors of MACE in multivariate analysis. We therefore analysed changes in roughness and PSS on a detailed frame-by-frame basis in peri-MLA segments. Plaques exhibited marked changes in roughness over a few frames, and this was particularly seen in MACE vs. no-MACE lesions (*Figure 5*). Importantly, while roughness and

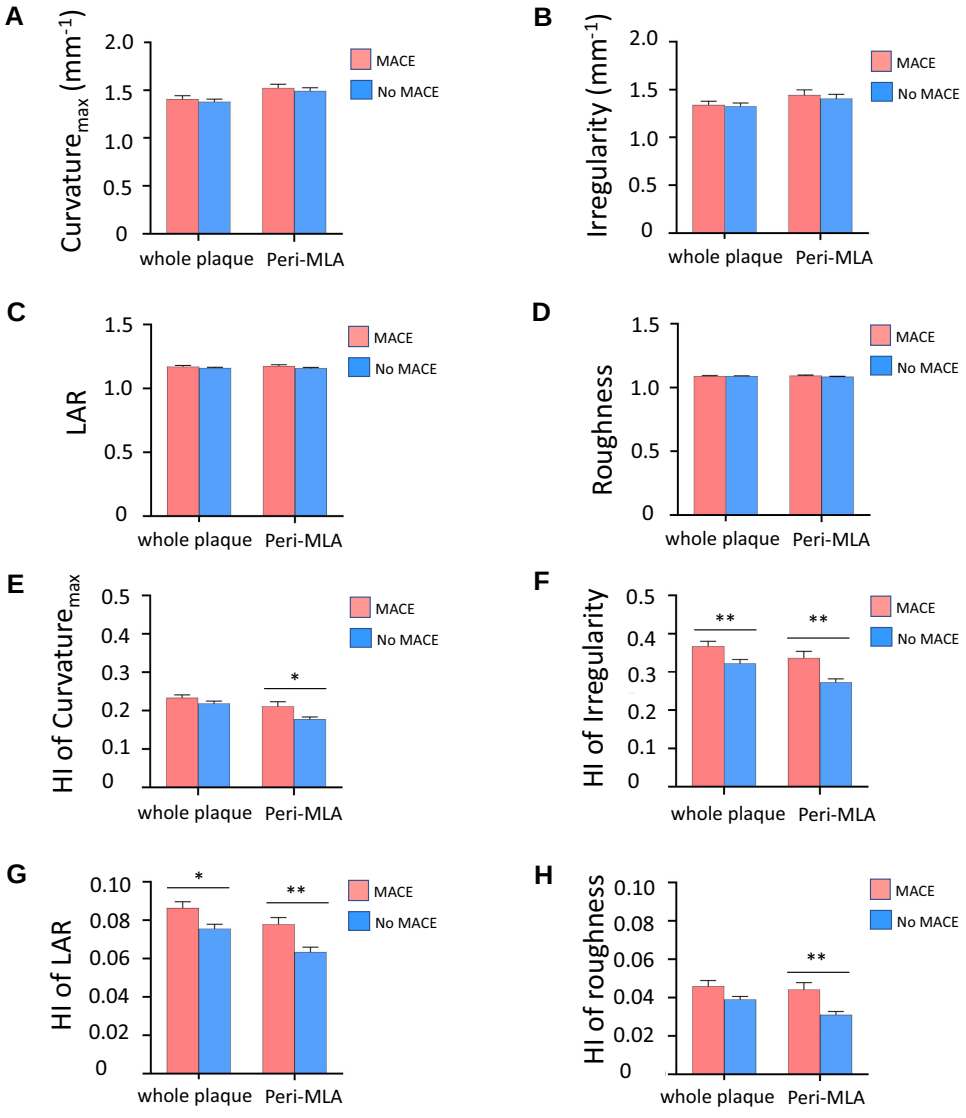

Figure 3 Plaque–lumen geometric parameters and their heterogeneity in major adverse cardiovascular events and no-major adverse cardiovascular events plaques. (*A*) Maximum lumen curvature, (*B*) irregularity, (*C*) lumen aspect ratio, and (*D*) lumen roughness, or heterogeneity index of (*E*) maximum lumen curvature, (*F*) irregularity, (*G*) lumen aspect ratio, and (*H*) lumen roughness in major adverse cardiovascular events and no-major adverse cardiovascular events plaques. Data are means (standard error) for (*A–D*) and means (standard deviation) for (*E–H*), *$P < 0.05$; **$P < 0.01$. HI, heterogeneity index; LAR, lumen aspect ratio; other abbreviations as in *Figure 1*.

PSS curves often followed the same patterns across the lesion, they were markedly discordant over some frames, again particularly in MACE vs. no-MACE lesions. This suggests that geometric parameters exert their effects on plaques only in part through PSS.

Incorporating peri-minimal luminal area heterogeneity roughness improves prediction of major adverse cardiovascular events

These geometric parameters measure unevenness of the plaque–lumen interface and circumferential curvature and are thus largely independent of conventional imaging parameters used to define higher risk plaques; we therefore examined whether these geometric parameters increase prediction of NCL MACE in VH-IVUS-defined higher risk lesions. We focused on HI roughness since it showed high specificity while maintaining high sensitivity. Incorporating peri-MLA roughness heterogeneity (optimal cut-off = 0.035) improved prediction of NCL MACE (*Figure 6A–D*) for plaques with MLA ≤ 4 mm^2 ($P < 0.001$), PB $\geq 70\%$ ($P < 0.001$), and VH-TCFAs ($P < 0.001$), but not for VH-TCFA with PB $\geq 70\%$ ($P = 0.081$). High HI PSS increased the predictive ability of PSS on NCL MACE in plaques with PB $\geq 70\%$, MLA ≤ 4 mm^2, and VH-TCFA.[18] Including HI roughness further increased NCL MACE prediction in high PSS plaques both alone and with other features (*Figure 6E–H*), including all plaques ($P < 0.001$),

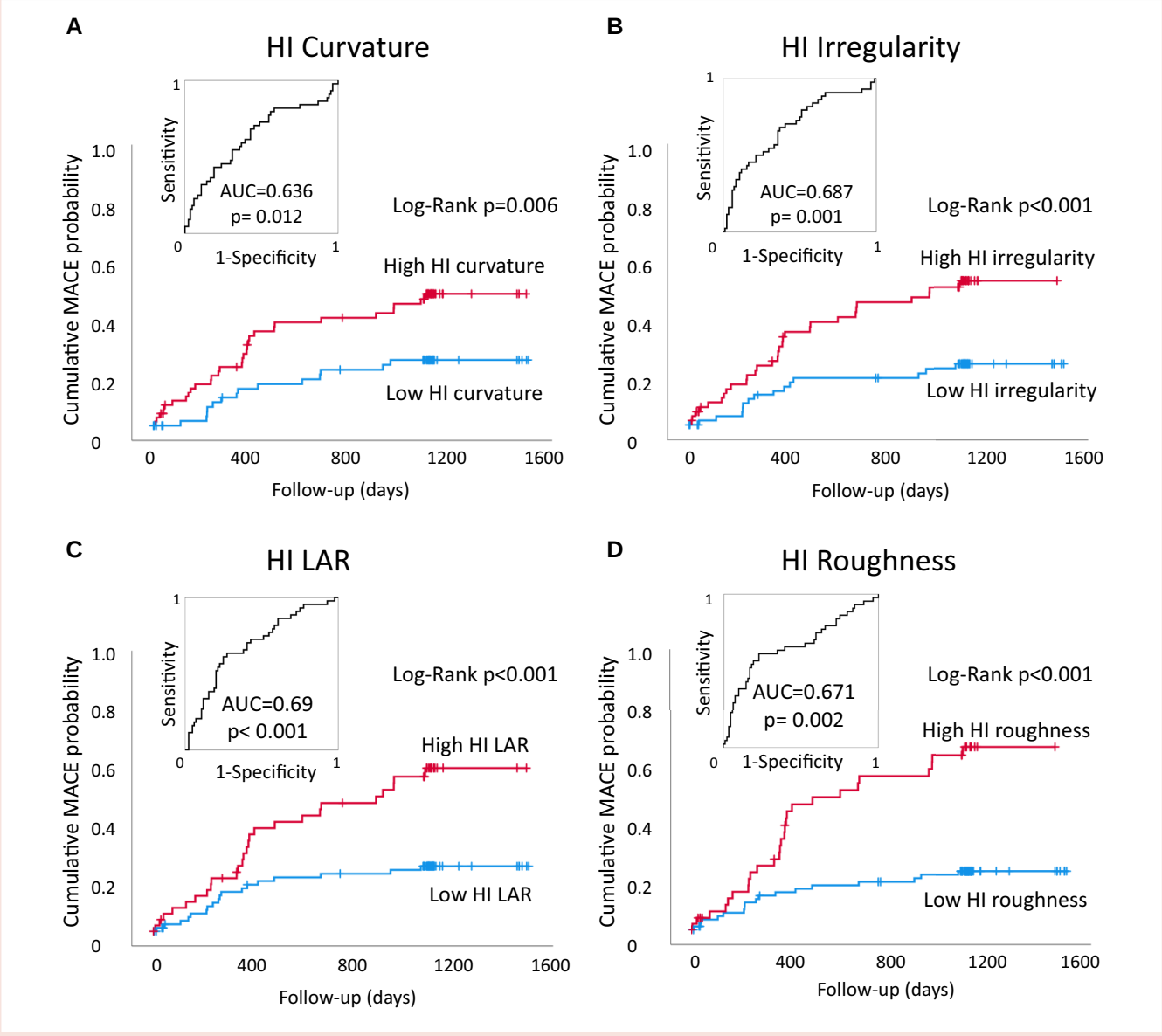

Figure 4 Time-to-event curves according to peri-minimal luminal area heterogeneity and respective receiver operating characteristic curves. Cumulative major adverse cardiovascular events probability according to high or low heterogeneity index of (*A*) curvature, (*B*) irregularity, (*C*) lumen aspect ratio, and (*D*) roughness. AUC, area under curve; ROC, receiver operating characteristic; other abbreviations as in *Figures 1* and *3*.

Table 1 Univariate and multivariate plaque-based analyses of associations between peri-minimal luminal area geometric heterogeneity indices and major adverse cardiovascular events

Peri-MLA segments	Univariate model		Multivariate model	
	HR (95% CI)	*P*	HR (95% CI)	*P*
HI $curvature_{max}$	2.38 (1.26–4.50)	**0.007**	—	—
HI irregularity	2.89 (1.53–5.46)	**0.001**	—	—
HI LAR	3.01 (1.65–5.50)	**<0.001**	—	—
HI roughness	4.12 (2.23–7.61)	**<0.001**	3.21 (1.70–6.05)	**<0.001**
HI PSS_{max}	3.57 (1.91–6.66)	**<0.001**	2.67 (1.40–5.10)	**0.003**

Bold values indicate statistical significance ($P < 0.05$).
CI, confidence interval; HI, heterogeneity index; HR, hazard ratio; LAR, lumen aspect ratio; MACE, major adverse cardiovascular events; MLA, minimal luminal area.

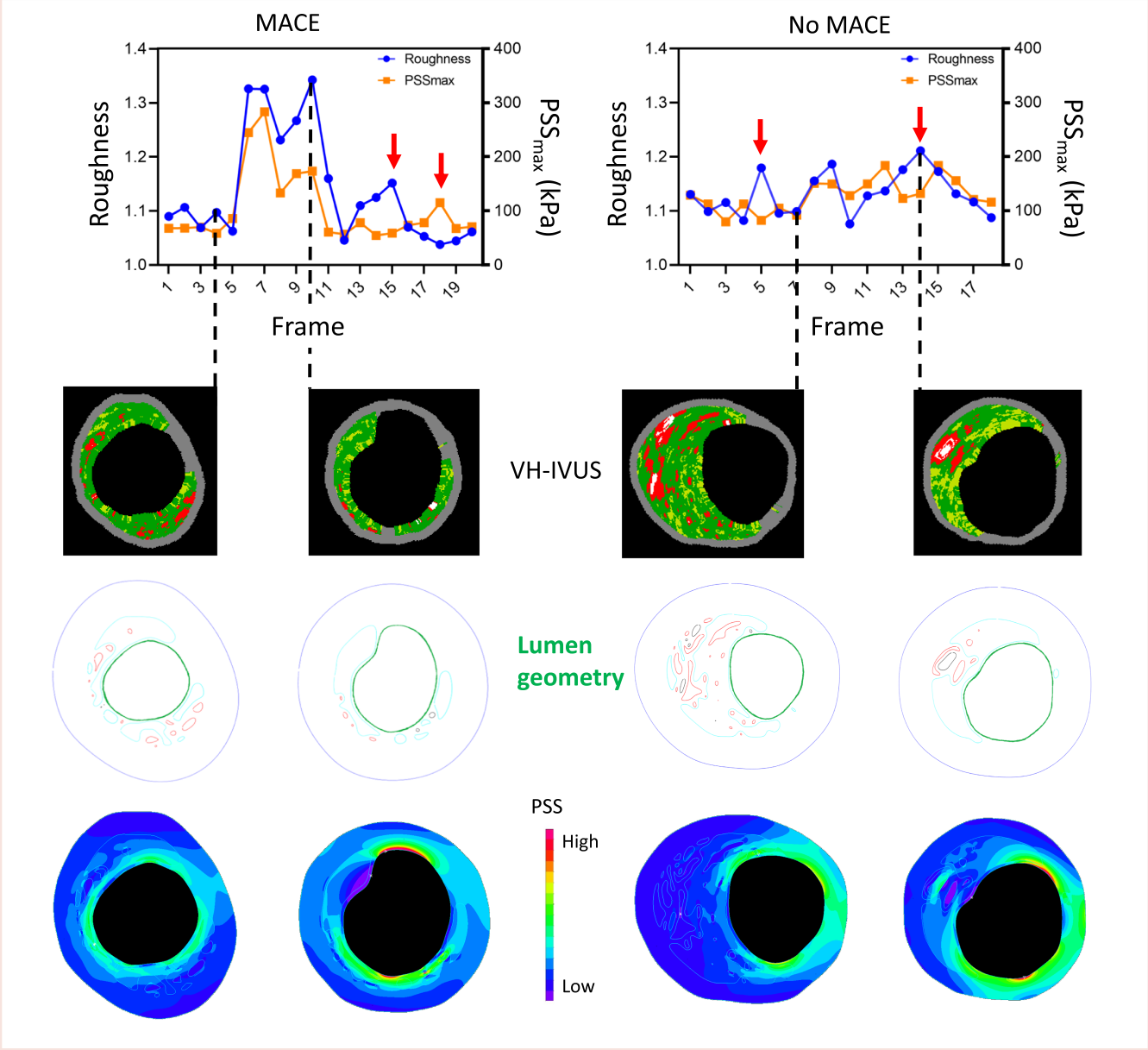

Figure 5 Longitudinal variation in plaque–lumen geometry. Graphs of roughness and plaque structural stress across 18–20 peri-minimal luminal area frames of major adverse cardiovascular events plaque (left) or no-major adverse cardiovascular events plaque (right) showing higher heterogeneity index roughness in major adverse cardiovascular events plaque. Arrows highlight the discordant areas in roughness and plaque structural stress. Panels below show selected virtual histology intravascular ultrasound frames, lumen segmentation (highlighted in thicker line) and plaque structural stress band plots. PSS, plaque structural stress; other abbreviations as in *Figure 1*.

VH-TCFAs ($P = 0.008$), MLA ≤ 4 mm^2 ($P = 0.047$), and PB $\geq 70\%$ ($P = 0.003$). Including HI roughness increased the PPV compared with imaging alone from 36.6 to 58.7% for all plaques, 36.5 to 61.9% for VH-TCFAs, 39 to 73.3% for MLA ≤ 4 mm^2, 35.7 to 63.2% for PB $\geq 70\%$, and these were comparable to using combined PSS and HI PSS (all plaques = 60.6%, VH-TCFA = 63.6%, MLA$\leq$4 mm^2 = 66.7%, PB $\geq 70\%$ = 56.3%).[18]

Features contributing to luminal roughness and heterogeneity

PROSPECT used grey-scale and VH-IVUS to identify plaques at higher risk of MACE. However, neither modality has sufficient resolution to identify some features that underlie geometric heterogeneity. We therefore undertook an exploratory analysis using co-registered baseline VH-IVUS and OCT images from 53 plaques from the Integrated Biomarkers Imaging Study-4[19] (see Supplementary material online, *Figure S1*). High HI roughness (threshold as above) was identified from 1319 VH-IVUS frames, and regions of interest, particularly peri-MLA segments, then identified on co-registered 2517 OCT frames from the same patient. High HI roughness was particularly associated with specific features on OCT, including multi-layered appearances (80 vs. 37.2%, $P = 0.031$, Supplementary material online, *Table S4* and Supplementary material online, *Figure S2*) and calcification protruding into the lumen.

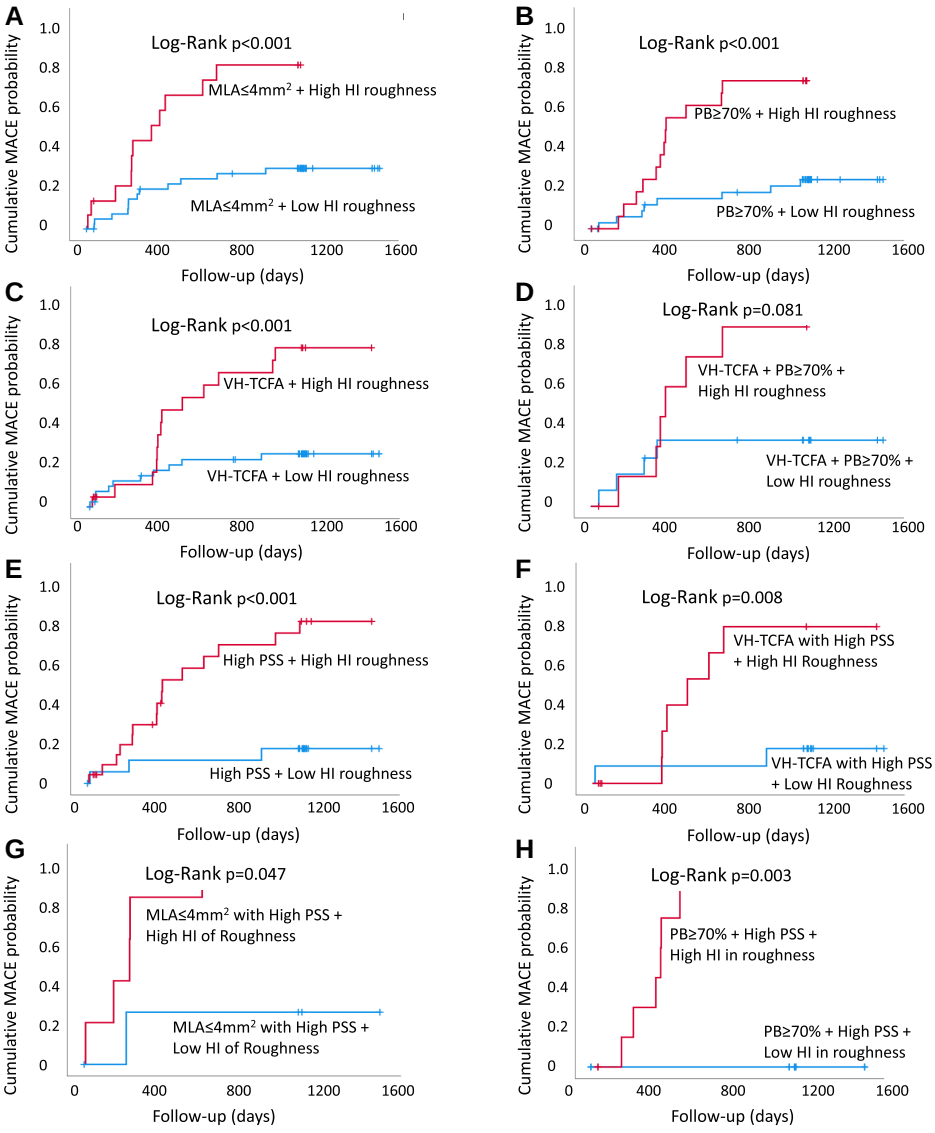

Figure 6 Time-to-event curves according to plaque plaque structural stress and roughness heterogeneity groups. Cumulative major adverse cardiovascular events probability according to high or low peri-minimal luminal area roughness heterogeneity for (*A*) plaques with minimal luminal area ≤ 4 mm^2, (*B*) plaque burden ≥ 70%, (*C*) virtual histology thin-cap fibroatheroma, (*D*) virtual histology thin-cap fibroatheroma + plaque burden ≥ 70%, (*E*) high plaque structural stress, (*F*) virtual histology thin-cap fibroatheroma + high plaque structural stress, (*G*) minimal luminal area ≤ 4 mm^2 + high plaque structural stress, (*H*) plaque burden ≥ 70% + high plaque structural stress. VH-TCFA, virtual histology thin-cap fibroatheroma; other abbreviations as in *Figures 1* and *5*.

Discussion

We analysed a range of geometric parameters describing the plaque–lumen interface in a *post-hoc* sub-group analysis of 44 MACE and 84 propensity-matched no-MACE-NCL plaques from PROSPECT. We find: (i) plaque geometric parameters are more heterogeneous in MACE vs. no-MACE-NCLs, across both the whole plaque and peri-MLA segments; (ii) high peri-MLA HI roughness is an independent predictor of future MACE; (iii) incorporating HI roughness improves risk stratification of higher risk plaques detected by VH-IVUS, and further improves risk prediction by PSS; (iv) geometric parameters show high heterogeneity associated with specific plaque features, including multi-layered plaque and calcification protruding into the lumen. Our data suggest that incorporating geometric parameters may improve ability of coronary imaging to detect higher risk plaques that lead to MACE.

Risk stratification of coronary plaques aims to identify features associated with plaque progression and destabilization, and prospective natural history studies have identified higher risk features (e.g. PB, MLA, TCFAs) or composition (e.g. lipid arc/pool). However, low overall event rates suggest that factors additional to plaque size, stenosis, and composition determine plaque instability and growth, and a holistic approach assessing both systemic and 'local' risk, including biomarkers, plaque features, and biomechanical parameters, is recommended.[20,21]

PSS measurements integrate effects of plaque anatomy and composition with physical forces, and including PSS improves MACE prediction,[18,22] especially in higher risk regions. However, PSS calculation needs expert analysis with high computational requirements, and plaques are complex structures with many different components, shapes, and sizes, resulting in marked heterogeneity of plaque structure, geometry, and PSS along their length.[18] In contrast, PSS correlates with lumen curvature, irregularity, and roughness, which measure both large and small lumen/plaque irregularities, and can be determined on a standard computer. Simulation times for geometric parameters were much shorter than for PSS (11.5 vs. 190 min), making fast, automated, real-time assessment achievable. Therefore, this would make geometric parameters attractive surrogate markers of PSS.

One aim of plaque imaging is to target local or systemic therapy according to prognosis. While the benefits of higher risk plaque-driven management are unproven, such an approach is the subject of a number of recent clinical trials. For example, PROSPECT-ABSORB examined pre-emptive stenting of non-flow-limiting vulnerable plaques, and showed an increase in MLA at follow-up was associated with favourable clinical outcomes.[23] However, the benefits of prophylactic stenting of higher risk NCLs depend upon their risk of MACE, which is determined currently by coronary imaging. We show that heterogeneity of multiple geometric parameters is associated with MACE, and high HI roughness could increase the cumulative probability of MACE in plaques with different higher risk features (MLA ≤ 4 mm^2, PB $\geq 70\%$, VH-TCFA), with curves diverging mostly within 1 year of follow-up. While tortuosity of vessel segments is associated with ACS,[24] we show that heterogeneity of geometric features occurs over very short distances (4 mm proximal and distal to MLA). In addition, many MACE in PROSPECT were attributable to hospitalization due to progressive and unstable angina, which could be caused by plaque growth from sub-clinical silent ruptures and healing, which also change plaque geometry and structure.

We investigated whether the relationship between geometric heterogeneity and MACE was due to their effect on heterogeneity of PSS. High PSS determined by biomechanical modelling is associated with ACS presentation vs. stable patients,[25] and with plaque ruptures identified by OCT which were mostly silent.[15] The plaque–lumen geometric parameters and their heterogeneity affect PSS, which plays a pivotal role in both plaque growth and subsequent plaque disruption.[17] Plaque–lumen geometric measures and their longitudinal heterogeneity were positively correlated with PSS and its longitudinal heterogeneity, and curves of both roughness and PSS were often similar. However, PSS is also determined by plaque composition and haemodynamic factors, and roughness and PSS curves showed areas of discordance. Both HI roughness and HI PSS were also independently associated with MACE on multivariate analysis, and HI roughness improved risk stratification of high PSS plaques, both alone and with high-risk imaging features. These observations suggest that geometric parameters exert their effects only in part through PSS, and increased geometric heterogeneity coupled with high PSS could potentially promote plaque growth and destabilization.

The causes of heterogeneous geometry of the plaque–lumen interface are unclear, since VH-IVUS cannot detect subtle changes in the peri-luminal plaque which cause an uneven surface. We therefore explored the peri-luminal features that determine geometric heterogeneity using co-registered VH-IVUS and OCT images. Peri-MLA regions with high geometric heterogeneity were associated with a multi-layered appearance, similar to histological appearances consistent with repeated rounds of non-occlusive thrombus from plaque rupture/erosion and repair.[6,13] Thus, high longitudinal geometric heterogeneity could be both a cause and consequence of plaque disruption and rapid plaque growth. Similarly, calcified nodules account for up to 7% of acute MIs or sudden cardiac death,[1] and may partly exert this effect through high longitudinal geometric heterogeneity.

Our study has a number of clinical implications: (i) geometric assessment (for example HI roughness with an HR: 3.21 in the current study), offers quick, easy, and practical identification of higher risk plaques that improves the predictive ability of intravascular imaging; (ii) high geometric heterogeneity may also identify more moderate lesions that have or will undergo rapid plaque growth. Future studies should examine these predictions and particularly whether geometric heterogeneity identified by other imaging modalities are also associated with MACE.

Study limitations

Our study has several limitations. First, geometric assessment was performed retrospectively, and prospective studies are required to confirm the added value of plaque geometry and its heterogeneity in plaque risk assessment. However, propensity score matching ensured a well-matched control group for comparison. Second, VH-IVUS has well-documented limitations to identify and measure plaque components, including fibrous cap thickness that correlates negatively with PSS. However, the geometric parameters that segregate MACE vs. no-MACE (lumen curvature, irregularity, and roughness) are all within VH-IVUS resolution. Third, since geometric heterogeneity is based on lumen surface segmentation which may vary between imaging modalities, more research is needed to examine its value in other modalities such as grey-scale IVUS, OCT, and non-invasive techniques. Lastly, the relationship between wall shear stress (WSS) and plaque geometry was not investigated. Spatial heterogeneity of WSS profiles has been observed in patients,[26] but it is complex to compute, and further studies should examine the relationships between heterogeneity of plaque geometry and WSS with MACE.

Conclusion

We find that plaques leading to MACE have more heterogeneous longitudinal geometry of the plaque–lumen interface, both across the whole plaque and peri-MLA segments. Including geometric heterogeneity may improve the ability of intravascular imaging to predict MACE, suggesting that plaque geometric assessment may be important for coronary plaque risk stratification.

Lead author biography

Martin R. Bennett holds the British Heart Foundation (BHF) Chair of Cardiovascular Sciences at the University of Cambridge, directs the BHF Cambridge Centre for Cardiovascular Research Excellence, and holds Honorary Consultant Cardiologist positions at Cambridge University and Royal Papworth Hospitals. His clinical research programme combines clinical medicine, coronary imaging and engineering for vulnerable plaque detection.

Data availability

The data underlying this article will be shared on reasonable request to the corresponding author.

Supplementary material

Supplementary material is available at *European Heart Journal Open* online.

Funding

This work was funded by BHF grants FS/19/66/34658, PG/16/24/32090, RG71070, RG84554, the BHF Centre for Research Excellence (London, UK), and the National Institute of Health Research Cambridge Biomedical Research Centre (London, UK).

Conflict of interest: None declared.

References

1. Virmani R, Burke AP, Farb A, Kolodgie FD. Pathology of the vulnerable plaque. *J Am Coll Cardiol* 2006;**47**:C13–C18.
2. Bom MJ, van der Heijden DJ, Kedhi E, van der Heyden J, Meuwissen M, Knaapen P, Timmer SAJ, van Royen N. Early detection and treatment of the vulnerable coronary plaque: can we prevent acute coronary syndromes? *Circ Cardiovasc Imaging* 2017;**10**:e005973.
3. Stone GW, Maehara A, Lansky AJ, De Bruyne B, Cristea E, Mintz GS, Mehran R, McPherson J, Farhat N, Marso SP, Parise H, Templin B, White R, Zhang Z, Serruys PW. A prospective natural-history study of coronary atherosclerosis. *N Engl J Med* 2011;**364**:226–235.
4. Calvert PA, Obaid DR, O'Sullivan M, Shapiro LM, McNab D, Densem CG, Schofield PM, Braganza D, Clarke SC, Ray KK, West NEJ, Bennett MR. Association between IVUS findings and adverse outcomes in patients with coronary artery disease. *J Am Coll Cardiol Img* 2011;**4**:894–901.
5. Cheng JM, Garcia-Garcia HM, De Boer SPM, Kardys I, Heo JH, Akkerhuis KM, Oemrawsingh RM, Van Domburg RT, Ligthart J, Witberg KT, Regar E, Serruys PW, Van Geuns RJ, Boersma E. In vivo detection of high-risk coronary plaques by radiofrequency intravascular ultrasound and cardiovascular outcome: results of the ATHEROREMO-IVUS study. *Eur Heart J* 2014;**35**:639–647.
6. Vergallo R, Porto I, D'Amario D, Annibali G, Galli M, Benenati S, Bendandi F, Migliaro S, Fracassi F, Aurigemma C, Leone AM, Buffon A, Burzotta F, Trani C, Niccoli G, Liuzzo G, Prati F, Fuster V, Jang IK, Crea F. Coronary atherosclerotic phenotype and plaque healing in patients with recurrent acute coronary syndromes compared with patients with long-term clinical stability: an in vivo optical coherence tomography study. *JAMA Cardiol* 2019;**4**:321–329.
7. Prati F, Romagnoli E, Gatto L, La Manna A, Burzotta F, Ozaki Y, Marco V, Boi A, Fineschi M, Fabbiocchi F, Taglieri N, Niccoli G, Trani C, Versaci F, Calligaris G, Ruscica G, Di Giorgio A, Vergallo R, Albertucci M, Biondi-Zoccai G, Tamburino C, Crea F, Alfonso F, Arbustini E. Relationship between coronary plaque morphology of the left anterior descending artery and 12 months clinical outcome: the CLIMA study. *Eur Heart J* 2019;**41**:383–391.
8. Waksman R, Di Mario C, Torguson R, Ali ZA, Singh V, Skinner WH, Artis AK, Ten CT, Powers E, Kim C, Regar E, Wong SC, Lewis S, Wykrzykowska J, Dube S, Kazziha S, van der Ent M, Shah P, Craig PE, Zou Q, Kolm P, Brewer HB, Garcia-Garcia HM, Samady H, Tobis J, Zainea M, Leimbach W, Lee D, Lalonde T, Skinner W, Villa A, Liberman H, Younis G, de Silva R, Diaz M, Tami L, Hodgson J, Raveendran G, Goswami N, Arias J, Lovitz L, Carida R, Potluri S, Prati F, Erglis A, Pop A, McEntegart M, Hudec M, Rangasetty U, Newby D. Identification of patients and plaques vulnerable to future coronary events with near-infrared spectroscopy intravascular ultrasound imaging: a prospective, cohort study. *Lancet* 2019;**394**:1629–1637.
9. Tufaro V, Serruys PW, Räber L, Bennett MR, Torii R, Gu SZ, Onuma Y, Mathur A, Baumbach A, Bourantas CV. Intravascular imaging assessment of pharmacotherapies targeting atherosclerosis: advantages and limitations in predicting their prognostic implications. *Cardiovasc Res* 2023;**119**:121–135.
10. Refaat H, Niccoli G, Gramegna M, Montone RA, Burzotta F, Leone AM, Trani C, Ammar AS, Elsherbiny IA, Scalone G, Prati F, Crea F. Optical coherence tomography features of angiographic complex and smooth lesions in acute coronary syndromes. *Int J Cardiovasc Imaging* 2015;**31**:927–934.
11. Lee JM, Choi G, Hwang D, Park J, Kim HJ, Doh J-H, Nam C-W, Na S-H, Shin E-S, Taylor CA, Koo B-K. Impact of longitudinal lesion geometry on location of plaque rupture and clinical presentations. *J Am Coll Cardiol Imaging* 2017;**10**:677–688.
12. Kang D-Y, Ahn J-M, Kim YW, Moon JY, Lee JS, Koo B-K, Lee PH, Park D-W, Kang S-J, Lee S-W, Kim Y-H, Park S-W, Park S-J. Impact of coronary lesion geometry on fractional flow reserve: data from interventional cardiology research in-cooperation society-fractional flow reserve and intravascular ultrasound registry. *Circ Cardiovasc Imaging* 2018;**11**:e007087.
13. Fracassi F, Crea F, Sugiyama T, Yamamoto E, Uemura S, Vergallo R, Porto I, Lee H, Fujimoto J, Fuster V, Jang I-K. Healed culprit plaques in patients with acute coronary syndromes. *J Am Coll Cardiol* 2019;**73**:2253–2263.
14. Gu SZ, Costopoulos C, Huang Y, Bourantas C, Woolf A, Sun C, Teng Z, Losdat S, Räber L, Samady H, Bennett MR. High-intensity statin treatment is associated with reduced plaque structural stress and remodelling of artery geometry and plaque architecture. *Eur Hear J Open* 2021;**1**:oeab039.
15. Costopoulos C, Huang Y, Brown AJ, Calvert PA, Hoole SP, West NEJ, Gillard JH, Teng Z, Bennett MR. Plaque rupture in coronary atherosclerosis is associated with increased plaque structural stress. *J Am Coll Cardiol Img* 2017;**10**:1472–1483.
16. Gu SZ, Bennett MR. Plaque structural stress: detection, determinants and role in atherosclerotic plaque rupture and progression. *Front Cardiovasc Med* 2022;**9**:875413.
17. Costopoulos C, Timmins LH, Huang Y, Hung OY, Molony DS, Brown AJ, Davis EL, Teng Z, Gillard JH, Samady H, Bennett MR. Impact of combined plaque structural stress and wall shear stress on coronary plaque progression, regression, and changes in composition. *Eur Heart J* 2019;**40**:1411–1422.
18. Costopoulos C, Maehara A, Huang Y, Brown AJ, Gillard JH, Teng Z, Stone GW, Bennett MR. Heterogeneity of plaque structural stress is increased in plaques leading to MACE: insights from the PROSPECT study. *J Am Coll Cardiol Img* 2020;**13**:1206–1218.
19. Räber L, Taniwaki M, Zaugg S, Kelbæk H, Roffi M, Holmvang L, Noble S, Pedrazzini G, Moschovitis A, Lüscher TF, Matter CM, Serruys PW, Jüni P, Garcia-Garcia HM, Windecker S. Effect of high-intensity statin therapy on atherosclerosis in non-infarct-related coronary arteries (IBIS-4): a serial intravascular ultrasonography study. *Eur Heart J* 2015;**36**:490–500.
20. Tomaniak M, Katagiri Y, Modolo R, de Silva R, Khamis RY, Bourantas CV, Torii R, Wentzel JJ, Gijsen FJH, van Soest G, Stone PH, West NEJ, Maehara A, Lerman A, van der Steen AFW, Lüscher TF, Virmani R, Koenig W, Stone GW, Muller JE, Wijns W, Serruys PW, Onuma Y. Vulnerable plaques and patients: state-of-the-art. *Eur Heart J* 2020;**41**:2997–3004.
21. Dweck MR, Maurovich-Horvat P, Leiner T, Cosyns B, Fayad ZA, Gijsen FJH, Van der Heiden K, Kooi ME, Maehara A, Muller JE, Newby DE, Narula J, Pontone G, Regar E, Serruys PW, van der Steen AFW, Stone PH, Waltenberger JL, Yuan C, Evans PC, Lutgens E, Wentzel JJ, Bäck M. Contemporary rationale for non-invasive imaging of adverse coronary plaque features to identify the vulnerable patient: a position paper from the European Society of Cardiology Working Group on Atherosclerosis and Vascular Biology and the European Association of Cardiovascular Imaging. *Eur Hear J Cardiovasc Imaging* 2020;**21**:1177–1183.
22. Brown AJ, Teng Z, Calvert PA, Rajani NK, Hennessy O, Nerlekar N, Obaid DR, Costopoulos C, Huang Y, Hoole SP, Goddard M, West NEJ, Gillard JH, Bennett MR. Plaque structural stress estimations improve prediction of future Major adverse cardiovascular events after intracoronary imaging. *Circ Cardiovasc Imaging* 2016;**9**:e004172.
23. Stone GW, Maehara A, Ali ZA, Held C, Matsumura M, Kjøller-Hansen L, Bøtker HE, Maeng M, Engstrøm T, Wiseth R, Persson J, Trovik T, Jensen U, James SK, Mintz GS, Dressler O, Crowley A, Ben-Yehuda O, Erlinge D. Percutaneous coronary intervention for vulnerable coronary atherosclerotic plaque. *J Am Coll Cardiol* 2020;**76**:2289–2301.
24. Han D, Lin A, Kuronuma K, Tzolos E, Kwan AC, Klein E, Andreini D, Bax JJ, Cademartiri F, Chinnaiyan K, Chow BJW, Conte E, Cury RC, Feuchtner G, Hadamitzky M, Kim Y-J, Leipsic JA, Maffei E, Marques H, Plank F, Pontone G, Villines TC, Al-Mallah MH, de Araújo Gonçalves P, Danad I, Gransar H, Lu Y, Lee J-H, Lee S-E, Baskaran L, Al'Aref SJ, Yoon YE, Van Rosendael A, Budoff MJ, Samady H, Stone PH, Virmani R, Achenbach S, Narula J, Chang H-J, Min JK, Lin FY, Shaw LJ, Slomka PJ, Dey D, Berman DS. Association of plaque location and vessel geometry determined by coronary computed tomographic angiography with future acute coronary syndrome–causing culprit lesions. *JAMA Cardiol* 2022;**7**:309–319.
25. Teng Z, Brown AJ, Calvert PA, Parker RA, Obaid DR, Huang Y, Hoole SP, West NEJ, Gillard JH, Bennett MR. Coronary plaque structural stress is associated with plaque composition and subtype and higher in acute coronary syndrome: the BEACON i (biomechanical evaluation of atheromatous coronary arteries) study. *Circ Cardiovasc Imaging* 2014;**7**:461–470.
26. Varshney AS, Coskun AU, Siasos G, Maynard CC, Pu Z, Croce KJ, Cefalo NV, Cormier MA, Fotiadis D, Stefanou K, Papafaklis MI, Michalis L, VanOosterhout S, Mulder A, Madder RD, Stone PH. Spatial relationships among hemodynamic, anatomic, and biochemical plaque characteristics in patients with coronary artery disease. *Atherosclerosis* 2021;**320**:98–104.